contacts in going down a group, as described above.

It has been suggested that there are no "free" $SeCl_3^+$ ions in $(SeCl_3)(NbCl_6)$ and $(SeCl_3)(TaCl_6)$ because the Se–Cl stretch occurs at 405 cm^{-1} which is considered to be too low.[44] A $Tl_2Cl_9^{2-}$ type structure or an edge-bridging model ($Cl_3SbCl_2MCl_4$, M = Nb, Ta) were favored. In $(SeCl_3)(SbCl_6)$, ν_1 is found in the Raman spectrum of 407 cm^{-1}. In addition, the similar sizes of the elements niobium, tantalum, and antimony in the +5 oxidation state (effective ionic radii 0.65, 0.65, and 0.61 Å, respectively[45]) and the existence of the dimer $SbNbCl_{10}$[46] rather than a salt like $(NbCl_4)(SbCl_6)$ all suggest a similar basicity for the three hexachloro anions. One would therefore expect $(SeCl_3)(NbCl_6)$ and $(SeCl_3)(TaCl_6)$ to contain the $SeCl_3^+$ ion. There may however be slightly stronger interionic interactions in the latter compounds.

Acknowledgment. We thank the Natural Sciences and Engineering Research Council of Canada for financial support of this work.

Registry No. $(SCl_3)(SbCl_6)$, 36487-44-2; $(SeCl_3)(SbCl_6)$, 16460-43-8; $(TeCl_3)(SbCl_6)$, 16460-42-7; $(TeCl_3)(AlCl_4)$, 36570-59-9; $(TeCl_3)(AsF_6)$, 19709-82-1; $(TeCl_3)(SbF_6)$, 99583-55-8; $(TeF_3)_2(SO_4)$, 99583-56-9; $(TeCl_3)(NbCl_6)$, 24494-45-9; As_4S_4, 12279-90-2; SbF_5, 7647-18-9; As, 7440-38-2; Se, 7782-49-2; $SeCl_4$, 10026-03-6; S, 7704-34-9; Br_2, 7726-95-6; Te, 13494-80-9; $AlCl_3$, 7446-70-0; S_7TeCl_2, 27669-14-3; AsF_5, 7784-36-3; $TeCl_4$, 10026-07-0; SO_2, 7446-09-5.

Supplementary Material Available: Tables IX–XXI containing complete bond lengths and bond angles for $(SCl_{1.2}Br_{1.8})(SbCl_6)$, $(SeCl_3)(SbCl_6)$, $(TeCl_3)(AlCl_4)$, $(TeCl_3)(AsF_6)$, $(TeCl_3)(SbF_6)$, and $(TeF_3)_2SO_4$ and anisotropic thermal parameters and final structure factor amplitudes for each compound and supplementary Figures 7–13 showing the crystal packing in $(SCl_3)(SbCl_6)$, $(SCl_{1.2}Br_{1.8})(SbCl_6)$, α- and β-$(TeCl_3)(AlCl_4)$, $(TeCl_3)(AsF_6)$, $(TeCl_3)(SbF_6)$, and $(TeF_3)_2(SO_4)$ (76 pages). Ordering information is given on any current masthead page.

(44) Poulsen, F. W.; Berg, R. W. *J. Inorg. Nucl. Chem.* **1978**, *40*, 471.
(45) Huheey, J. E. "Inorganic Chemistry: Principles of Structure and Reactivity"; 2nd ed., Harper and Row; New York, 1972.
(46) Bues, W.; Demiray, A. F.; Brockner, W. *Spectrochim. Acta, Part A* **1976**, *32A*, 1623.
(47) The periodic group notation in parentheses is in accord with recent actions by IUPAC and ACS nomenclature committees. A and B notation is eliminated because of wide confusion. Groups IA and IIA become groups 1 and 2. The d-transition elements comprise groups 3 through 12, and the p-block elements comprise groups 13 through 18. (Note that the former Roman number designation is preserved in the last digit of the new numbering: e.g., III → 3 and 13.)

Contribution from the Department of Chemistry, College of Arts and Sciences, The University of Tokyo, Komaba, Megruo, Tokyo 153, Japan

Crystal Structures of (α,ω-Diaminoalkane)cadmium(II) Tetracyanonickelate(II)–Aromatic Molecule Inclusion Compounds. 3. (1,4-Diaminobutane)cadmium(II) Tetracyanonickelate(II)–Pyrrole (1/1), (1,4-Diaminobutane)cadmium(II) Tetracyanonickelate(II)–Aniline (2/3), and (1,4-Diaminobutane)cadmium(II) Tetracyanonickelate(II)–*N*,*N*-Dimethylaniline (1/1)

Shin-Ichi Nishikiori and Toschitake Iwamoto*

Received June 24, 1985

The crystal structures of three inclusion compounds of pyrrole (**1**), aniline (**2**), and *N*,*N*-dimethylaniline (**3**), each of the aromatics being accommodated respectively as the guest in the three-dimensional metal complex host structure of (1,4-diaminobutane)-cadmium(II) tetracyanonickelate(II), have been determined by X-ray diffraction methods. Compound **1**, $Cd[NH_2(CH_2)_4NH_2]Ni(CN)_4 \cdot C_4H_5N$, crystallizes in the monoclinic space group $P2/m$, with the lattice parameters a = 7.840 (4) Å, b = 7.634 (2) Å, c = 7.060 (2) Å, β = 90.15 (6)°, and Z = 1; the final conventional R = 0.046 has been obtained for 1488 reflections. Compound **2**, $Cd[NH_2(CH_2)_4NH_2]Ni(CN)_4 \cdot 1.5C_6H_5NH_2$, crystallizes in the triclinic system $P\bar{1}$, with a = 9.774 (3) Å, b = 13.918 (8) Å, c = 7.715 (4) Å, α = 90.41 (4)°, β = 90.43 (5)°, γ = 93.18 (4)°, and Z = 2; final R = 0.066 for 2982 reflections. Compound **3**, $Cd[NH_2(CH_2)_4NH_2]Ni(CN)_4 \cdot C_6H_5N(CH_3)_2$, is monoclinic, $P2_1/m$, with a = 9.860 (5) Å, b = 15.267 (6) Å, c = 7.309 (4) Å, β = 113.92 (4)°, and Z = 2; final R = 0.057 for 3126 reflections. The substantial feature of the host structure common to these three inclusion compounds is its three-dimensional framework built by the stacking of two-dimensionally extended *cate-na*-[cadmium(II) tetrakis(μ-cyano)nickelate(II)] sheets and the ambident bridging of 1,4-diaminobutane ligands between the adjacent cyanometal complex sheets at each cadmium atom; the cadmium atom is six-coordinated by nitrogen atoms by four N ends of the CN^- groups and two N ends of the two 1,4-diaminobutane ligands in a trans configuration. The flexibility of the host structures is observed in the manner of waving of the two-dimensional cyanometal complex sheet and in the skeletal conformation of the bridging 1,4-diaminobutane ligand, both the manner of waving and the conformation being dependent on the geometry of the guest molecule.

Introduction

The three-dimensional metal complex (α,ω-diaminoalkane)-cadmium(II) tetracyanonickelate(II) accommodates several kinds of aromatic molecules as guests to give a series of inclusion compounds.[1] The series have been derived from the Hofmann-type clathrate $Cd(NH_3)_2Ni(CN)_4 \cdot 2G$ (G = C_4H_4S, C_4H_5N, C_6H_6, C_6H_5OH, or $C_6H_5NH_2$).[2] In order to increase the inclusion ability of the metal complex host for substituted aromatic molecules bulkier than those designated as G in the formula, the pair of ammine ligands protruding from adjacent square-planar cadmium(II) tetracyanonickelate(II) sheets were replaced by the α,ω-diaminoalkane. The crystal structures of (1,4-diaminobutane)cadmium(II) tetracyanonickelate(II)–2,5-xylidine (1/1)[3] and (1,6-diaminohexane)cadmium(II) tetracyanonickelate(II)–*o*-toluidine (1/1)[4] were analyzed to demonstrate the inclusion structure of these compounds. As tabulated in ref 1 and 3, the guest molecules accommodated into the (diaminoalkane)cadmium(II) tetracyanonickelate(II) hosts are diverse in geometry: they range from pyrrole to 2,4,6-trimethylaniline and 1,2,3,4-tetramethylbenzene. The coefficient n of the guest molecule G in the general formula Cd(diaminoalkane)$Ni(CN)_4 \cdot nG$ varies from 1 to 2, but no distinct correlation has been observed between the

(1) Hasegawa, T. Nishikiori, S.; Iwamoto, T. *J. Inclusion Phenom.* **1983**, *1*, 365.
(2) Iwamoto, T. In "Inclusion Compounds"; Atwood, J. L., Davies, J. E. D., MacNicol, D. D., Eds.; Academic Press: London, 1984; Vol. 1, pp 29–57.
(3) Nishikiori, S.; Iwamoto, T. *J. Inclusion Phenom.* **1985**, *2*, 341.
(4) Hasegawa, T.; Nishikiori, S.; Iwamoto, T. *J. Inclusion Phenom.* **1984**, *2*, 351.

0020-1669/86/1325-0788$01.50/0

Table I. Crystallographic Data[a]

	1	2	3
formula	$C_{12}H_{17}N_7CdNi$	$C_{17}H_{22.5}N_{7.5}CdNi$	$C_{16}H_{23}N_7CdNi$
fw	430.41	503.02	484.51
color and habit	yellow plate	yellow plate	yellow plate
cryst syst	monoclinic	triclinic	monoclinic
space group	$P2/m$	$P\bar{1}$	$P2_1/m$
a/Å	7.840 (4)	9.774 (3)	9.860 (5)
b/Å	7.634 (2)	13.918 (8)	15.267 (6)
c/Å	7.060 (2)	7.715 (4)	7.309 (4)
α/deg	90	90.41 (4)	90
β/deg	90.15 (6)	90.43 (5)	113.92 (4)
γ/deg	90	93.18 (4)	90
V/Å^3	422.5 (2)	1047.8 (9)	1005.7 (8)
Z	1	2	2
D_m/g cm^{-3} [b]	1.67 (1)	1.61 (1)	1.61 (1)
D_c/g cm^{-3}	1.69	1.59	1.61
cryst size/mm	0.10 × 0.10 × 0.14	0.18 × 0.18 × 0.13	0.18 × 0.18 × 0.15
diffractometer	Rigaku AFC-6A	Rigaku AFC-6A	Rigaku AFC-6
radiation	Mo Kα (λ = 0.709 26 Å)	Mo Kα (λ = 0.709 26 Å)	Mo Kα (λ = 0.709 26 Å)
monochromator	graphite cryst, incident beam	graphite cryst, incident beam	graphite cryst, incident beam
μ(Mo Kα)/cm^{-1}	23.6	19.2	20.1
scan mode	2θ–ω	2θ–ω	2θ–ω
2θ scan range/deg	$2 < 2\theta < 70$	$2 < 2\theta < 50$	$2 < 2\theta < 67$
scan rate/deg min^{-1}	4	4	4
peak scan width	1.5 + 0.5 tan θ	1.4 + 0.5 tan θ	1.4 + 0.5 tan θ
collcn range	$-12 \le h \le 0$	$-11 \le h \le 11$	$-10 \le h \le 15$ [c]
	$-12 \le k \le 0$	$-16 \le k \le 16$	$-23 \le k \le 0$
	$-11 \le l \le 11$	$0 \le l \le 9$	$-10 \le l \le 11$
no. of reflcns collcd			
total no.	2105	4135	4440
no. used ($>3\sigma(F_o)$) ($N_{observn}$)	1488	2982	3126
no. of refined params (N_{param})	54	212	104
R,[d] R_w[e]	0.046, 0.042	0.066, 0.075	0.057, 0.048
S[f]	0.563	1.834	0.856
wt scheme (w)	$(77/F_o)^2$ for $\lvert F_o\rvert > 77$	$(50/F_o)^2$ for $\lvert F_o\rvert > 50$	$(100/F_o)^2$ for $\lvert F_o\rvert > 100$
	1 for $77 \ge \lvert F_o\rvert \ge 37$	1 for $50 \ge \lvert F_o\rvert \ge 25$	1 for $100 \ge \lvert F_o\rvert \ge 50$
	0.25 for $\lvert F_o\rvert < 37$	0.25 for $\lvert F_o\rvert < 25$	0.25 for $\lvert F_o\rvert < 50$

[a] **1** = $Cd(C_4H_{12}N_2)Ni(CN)_4{\cdot}C_4H_5N$, **2** = $Cd(C_4H_{12}N_2)Ni(CN)_4{\cdot}1.5C_6H_5NH_2$, and **3** = $Cd(C_4H_{12}N_2)Ni(CN)_4{\cdot}C_6H_5N(CH_3)_2$. [b] Measured by the flotation method in a bromoform–mesitylene mixture. [c] The setting of the axes was converted to the listed one after the collection of intensity data of **3**. [d] $R = \sum(||F_o| - |F_c||)/\sum|F_o|$. [e] $R_w = [\sum w(|F_o| - |F_c|)^2/\sum w(F_o)^2]^{1/2}$. [f] $S = [\sum w(|F_o| - |F_c|)^2/(N_{observn} - N_{param})]^{1/2}$.

value of n and the geometry of the guest molecule. These observations suggest that the compounds in this series are not isomorphous with each other, although their powder X-ray diffraction patterns show the presence of a systematic layered structure in common to them.[1,3] They may thus be comparable to the Hofmann-type and analogous series so far investigated by the present authors and co-workers, which are isostructural.[2] Therefore, it is necessary to determine crystal structures of representative members in this series in order to understand their structural features. Three members were chosen among the Hofmann-dabn-type $Cd(dabn)Ni(CN)_4{\cdot}nG$ (dabn = $NH_2(CH_2)_4NH_2$, 1,4-diaminobutane):[3] the pyrrole compound **1** (the smallest guest with n = 1), the aniline compound **2** (a monosubstituted guest with less bulky amino group but with n = 1.5), and the *N*,*N*-dimethylaniline compound **3** (a monosubstituted one with a bulkier dimethylamino group and n = 1). Their structures are compared with each other and with that of the 2,5-xylidine compound, the structure of which was reported previously.[3] In these Hofmann-dabn-type inclusion compounds each of the metal complex hosts has substantially the same three-dimensional structure, which is flexible enough to accommodate guest molecules different in size and shape; the guest molecules of **1** and **3** are disordered in the ordered host.

Experimental Section

General Information. The single crystals of the pyrrole, the aniline, and the *N*,*N*-dimethylaniline compounds were prepared by the method described previously.[1,3] The chemical compositions were ascertained by the elemental analyses for the pyrrole compound **1** as $Cd(C_4H_{12}N_2)Ni(CN)_4{\cdot}C_4H_5N$, for the aniline compound **2** as $Cd(C_4H_{12}N_2)Ni(CN)_4{\cdot}1.5C_6H_5NH_2$, and for the *N*,*N*-dimethylaniline compound **3** as $Cd(C_4H_{12}N_2)Ni(CN)_4{\cdot}C_6H_5N(CH_3)_2$.

Each crystal subjected to the X-ray diffraction experiments was coated with epoxy resin in order to prevent spontaneous decomposition under ambient atmosphere. After preliminary Weissenberg photographs were taken, the refinements of lattice parameters and the collections of intensity data were carried out on an automated four-circle Rigaku AFC-6A diffractometer with graphite-monochromated Mo Kα radiation at room temperature. The intensity data were corrected for Lorentz and polarization effects but not for absorption and extinction. The structure solution and the refinement of the parameters were achieved by the ordinary heavy-atom method, successive Fourier syntheses, and block-diagonal least-squares processes. All the calculations were performed on a HITAC M-280H computer at the Computation Center of the University of Tokyo using the programs in UNICSIII[5] including ORTEP,[6] and their local versions. The atomic scattering factors including those for real and imaginary dispersion corrections were taken from ref 7. Agreement factors (af) for multiply measured reflections in the all octants within the range $20° < 2\theta < 26°$ for **1** (240 reflections), $20° < 2\theta < 25°$ for **2** (494 reflections), and $20° < 2\theta < 25°$ for **3** (456 reflections) were checked and used for diagnosis of the point group.

The crystallographic and experimental data are summarized in Table I for **1**, **2**, and **3**. The results of the structure refinements have been deposited as supplementary material.

Pyrrole Compound (1). Among the three space groups $P2/m$, $P2$ and Pm suggested from the Laue symmetry observed on the preliminary Weissenberg photographs, $P2/m$ was chosen. The six af's ranging from 0.0133 to 0.0168 did not show any features characteristic to 2 and m point groups; refinement carried out in both $P2$ and Pm gave a few thermal parameters of dabn methylene carbons converging to negative values.

All atoms of the host except hydrogens were successively located on the Fourier and difference Fourier maps. The guest pyrrole molecule was

(5) Sakurai, T.; Kobayashi, K. *Rep. Inst. Phys. Chem. Res. (Jpn.)* **1979**, *55*, 69.
(6) Johnson, C. K. "ORTEP", Report ORNL-3794; Oak Ridge National Laboratory: Oak Ridge, TN, 1965.
(7) "International Tables for X-Ray Crystallography"; Kynoch Press: Birmingham, 1974; Vol. IV, pp 71–98, 148–151.

Table II. Final Atomic Parameters for **1**

	G^a	x/a	y/b	z/c	B_{eq}/Å$^{2\,b,c}$
Cd	0.25	0.0	0.0	0.0	1.80 (2)
Ni	0.25	0.0	0.5	0.5	2.25 (3)
C(1)	1.0	−0.0462 (5)	0.3277 (5)	0.3232 (5)	2.6 (1)
C(2)	0.5	0.3063 (8)	0.0	0.3289 (8)	3.9 (3)
C(3)	0.5	0.4919 (7)	0.0	0.3926 (7)	3.8 (3)
C(4)	0.25	0.594 (2)	0.5	0.048 (2)	5.0
C(5)	0.25	0.553 (2)	0.5	0.160 (2)	5.0
C(6)	0.25	0.671 (2)	0.5	−0.028 (2)	5.0
C(7)	0.25	0.401 (2)	0.5	0.178 (2)	5.0
N(1)	1.0	−0.0689 (5)	0.2191 (5)	0.2148 (5)	3.6 (1)
N(2)	0.5	0.2794 (6)	0.0	0.1224 (7)	3.4 (2)
H(1)^d	1.0	0.34463	0.11513	0.06186	5.0
H(2)	1.0	0.24493	0.11513	0.38568	5.0
H(3)	1.0	0.55625	0.11513	0.33726	5.0

^{a} G: multiplicity. ^{b} $B_{eq} = 4(\sum_i\sum_j B_{ij}a_ia_j)/3$. ^{c} The isotropic thermal parameters B was fixed at 5.0 Å^2 for C(4)–C(7) and for H(1)–H(3) in the refinement. ^{d} H(1) at N(2), H(2) at C(2), and H(3) at C(3).

placed on the mirror plane at $y/b = {}^1/_2$, but the electron cloud distributed around the $2/m$ site at $({}^1/_2, {}^1/_2, 0)$ was vague. Ultimately, four crystallographically independent peaks were recognized as the positions of the pyrrole skeletal atoms. Assuming that these peaks were due to the pyrrole molecule distributed statistically about the inversion center, $({}^1/_2, {}^1/_2, 0)$, each was given a 50% occupancy factor and included in the final refinement. All were assumed to be carbon; no discrimination of the N atom from the C atoms was possible. In the final stage the positional parameters for the non-hydrogen atoms of the host and guest and the anisotropic thermal parameters of the non-hydrogen host atoms were refined. The hydrogen atoms of the dabn were placed at calculated positions with isotropic thermal parameters of 5.0 Å^2, the same value applied to the isotropic thermal parameters of the guest atoms; these fixed parameters were included in the calculation of the F_c values. The final reliability indices were $R = 0.046$ and $R_w = 0.042$; the largest value of the ratio Δ/σ, where Δ is a parameter shift and σ is the estimated standard deviation of the parameter, was 0.2 for the parameters of the host atoms but approximately 1 for those of the guest atoms. Further improvement was impossible for the guest pyrrole molecule in the present refinement.

The final atomic coordinates determined are listed in Table II along with the isotropic equivalent thermal parameters.

Aniline Compound (2). During the data collection notable deviations of the standard reflections were observed: +1 to −2% for 020, +1 to −8% for 002, and 0 to +5% for 200. It appears that the samples was damaged by the X-ray irradiation. Since the deviations depended on direction in a complex manner, no corrections for the deviations were applied to the intensity data used in the structure analysis.

The centrosymmetric space group $P\bar{1}$ was chosen. The values of af calculated for the Bijvoet pairs of hkl and $h\bar{k}l$ with a monoclinic symmetry assumed were 0.0299 and 0.0339, respectively, significantly smaller than those for other pairs (0.1508–0.1593). Similar to the case of **1**, the atoms of the host constituents except hydrogens were located on the Fourier map. At this stage their positional and anisotropic thermal parameters were refined to $R = 0.084$ and $R_w = 0.107$; the positional parameters of hydrogen atoms fixed at the calculated positions with the isotropic thermal parameters fixed at 5.0 Å^2 were also included in the calculation of F_c values.

On the difference Fourier map two kinds of guest aniline molecules of considerably distorted shapes were found: G1 in one cavity centered at $({}^1/_2, {}^1/_4, 0)$, and G2 in another centered at $({}^1/_2, 0, {}^1/_2)$. Although the peaks associated with the G1 aniline were assigned to the skeletal atoms of an aniline molecule uniquely, those for G2 gave a more distorted shape than those of G1. Furthermore, the tentatively assigned atomic parameters diverged in the successive least-squares calculation. Therefore, only to the G1 skeletal atoms were anisotropic thermal parameters applied, and the positions of G2 were excluded from the final process of refinement. R and R_w went down to 0.066 and 0.075, respectively; the largest Δ/σ was 0.06 for the host constituents but exceeded 1 for G1. A torus elongated along the a axis (ca. 6.3 Å longer axis and ca. 6.0 Å shorter axis) and centered at $({}^1/_2, 0, {}^1/_2)$ with six peaks of 2.0–2.8 e Å^3 was seen on the final difference Fourier map; any improvement was attained in further refinement for G2 aniline molecule even by applying a rigid-group approximation. The atomic parameters determined are listed in Table III.

***N,N*-Dimethylaniline Compound (3).** Since the comparison of af values ranging from 0.0157 to 0.0289 supported the monoclinic crystal system but was ineffective for the decision of point group, the analysis

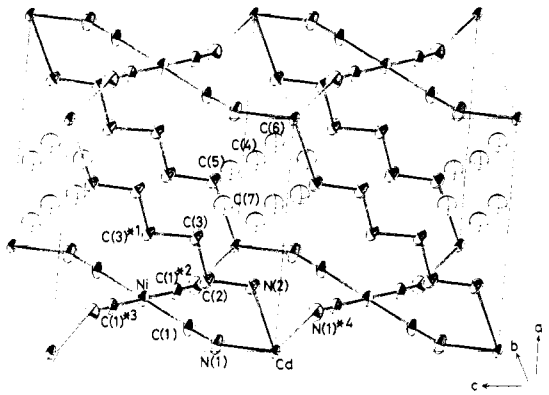

Figure 1. Perspective view of the structure of **1** with the numbering scheme. See the key to symmetry operations defined in Table V for the asterisked number. 30% thermal ellipsoids are shown for the host atoms and isotropic spheres of 5.0 Å^2 for the guest atoms; hydrogen atoms are omitted.

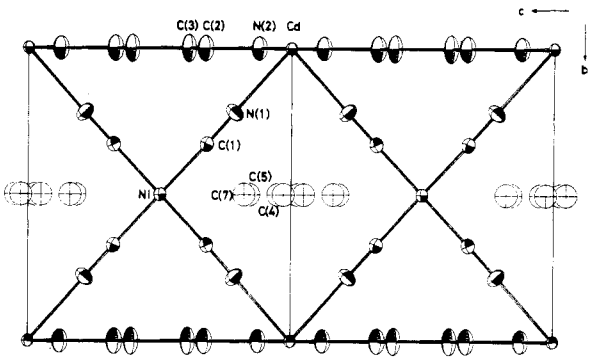

Figure 2. Projection of the structure of **1** along the a axis.

was initially undertaken in parallel with the two possible space groups $P2_1/m$ and $P2_1$. However, a significant difference in R was observed at the stage where the parameters of the guest molecules were included: $R = 0.074$ for $P2_1/m$, and $R = 0.080$ for the $P2_1$ space group. $P2_1/m$ was therefore adopted. With application of anisotropic thermal parameters to the non-hydrogen host atoms and isotropic ones fixed at 5.0 Å^2 to the hydrogen atoms of the dabn located at the calculated positions, the structure of the host framework was refined to $R = 0.074$ and $R_w = 0.064$. In the Fourier map of this stage, 13 peaks of electron density were observed in the cavity centered around the inversion center at $({}^1/_2, 0, 0)$. These peaks were assigned to the C and N atoms of a pair of *N,N*-dimethylaniline molecules statistically distributed about the inversion center with a 0.5 occupancy factor, although an unusual distortion of the skeletal structure appeared. In the final refinement, the isotropic thermal parameter fixed at 5.0 A^2 was applied to all the skeletal atoms of the guest molecule; the hydrogen atoms of the guest were not included in the least-squares calculations. Final values of $R = 0.057$ and $R_w = 0.048$ were obtained with the largest value of $\Delta/\sigma = 0.22$ for the host atoms, but some Δ/σ values for the guest atoms exceeded 1. In the final difference Fourier map, small peaks of electron density still remained in the area of the cavity. The atomic parameters are listed in Table IV.

Structure Descriptions

The structures determined are illustrated in Figures 1 and 2 for **1**, Figures 3 and 4 for **2**, and Figures 5 and 6 for **3** along with the atomic notations. Selected atomic distances and bond angles are listed in Tables V–VII for **1**–**3**, respectively; the least-squares planes for the aromatic ring of G1 aniline in **2** and of *N,N*-dimethylaniline in **3** are also included in Tables VI and VII, respectively.

The four Hofmann-dabn-type inclusion compounds, three in this paper and one in the previous one,[3] have essentially the same host structure: it is built of the two-dimensionally extended cadmium(II) tetracyanonickelate(II) sheets and of the 1,4-diaminobutane (dabn) ligands bridging the cadmium atoms in adjacent sheets. The cadmium atom thus exhibits six-coordination with four nitrogens of cyano groups and two nitrogens of two dabn groups. The two-dimensional cyanometal complex network is not planar but rather bent at every joint between the cadmium atom

Table III. Final Atomic Parameters for **2**

	G^a	x/a	y/b	z/c	$B_{eq}/Å^{2\,b,c}$
Cd	1.0	0.09521 (7)	0.26437 (5)	0.50349 (8)	2.00 (2)
Ni(1)	0.5	0.0	0.0	0.0	2.48 (6)
Ni(2)	0.5	0.0	0.5	0.0	2.19 (6)
C(1)	1.0	0.029 (1)	0.0923 (7)	0.173 (1)	3.0 (4)
C(2)	1.0	0.073 (1)	0.4259 (7)	0.173 (1)	2.6 (4)
C(3)	1.0	0.083 (1)	0.4286 (7)	0.831 (1)	2.7 (4)
C(4)	1.0	0.043 (1)	0.0915 (7)	0.831 (1)	3.1 (4)
C(15)	1.0	0.418 (1)	0.3204 (8)	0.513 (2)	3.8 (5)
C(6)	1.0	0.568 (1)	0.299 (1)	0.494 (2)	4.4 (5)
C(7)	1.0	0.664 (1)	0.3856 (9)	0.522 (2)	4.5 (6)
C(8)	1.0	0.814 (1)	0.371 (1)	0.480 (2)	5.0 (6)
C(9)	1.0	0.449 (3)	0.245 (3)	−0.011 (3)	18 (2)
C(10)	1.0	0.549 (3)	0.183 (2)	−0.045 (3)	10 (1)
C(11)	1.0	0.678 (3)	0.203 (3)	−0.033 (3)	15 (2)
C(12)	1.0	0.747 (4)	0.283 (2)	−0.009 (3)	13 (2)
C(13)	1.0	0.654 (4)	0.361 (2)	0.024 (3)	12 (2)
C(14)	1.0	0.508 (4)	0.350 (2)	0.031 (3)	13 (2)
N(1)	1.0	0.048 (1)	0.1479 (6)	0.279 (1)	4.5 (5)
N(2)	1.0	0.115 (1)	0.3799 (7)	0.283 (1)	3.5 (4)
N(3)	1.0	0.130 (1)	0.3840 (7)	0.724 (1)	3.6 (4)
N(4)	1.0	0.069 (1)	0.1472 (7)	0.726 (1)	4.5 (5)
N(5)	1.0	0.3221 (9)	0.2386 (7)	0.485 (1)	4.0 (4)
N(6)	1.0	0.864 (1)	0.2861 (8)	0.539 (2)	5.7 (6)
N(7)	1.0	0.334 (3)	0.243 (3)	0.004 (3)	16 (2)
H(1)[d]	1.0	0.33969	0.21227	0.35318	5.0
H(2)	1.0	0.34559	0.18517	0.57520	5.0
H(3)	1.0	0.40157	0.34882	0.64085	5.0
H(4)	1.0	0.39414	0.37672	0.41925	5.0
H(5)	1.0	0.58276	0.27122	0.36448	5.0
H(6)	1.0	0.59126	0.24600	0.58711	5.0
H(7)	1.0	0.66014	0.40661	0.65423	5.0
H(8)	1.0	0.62985	0.44289	0.44022	5.0
H(9)	1.0	0.87627	0.43165	0.52635	5.0
H(10)	1.0	0.82416	0.36898	0.33636	5.0
H(11)	1.0	0.80682	0.22314	0.48741	5.0
H(12)	1.0	0.84533	0.28331	0.68437	5.0

[a] G: multiplicity. [b] $B_{eq} = 4(\sum_i\sum_j B_{ij}a_ia_j)/3$. [c] The isotropic thermal parameter B was fixed at 5.0 Å^2 for H(1)–H(12) in the refinement. [d] H(1) and H(2) at N(5), H(3) and H(4) at C(5), H(5) and H(6) at C(6), H(7) and H(8) at C(7), H(9) and H(10) at C(8), and H(11) and H(12) at N(6).

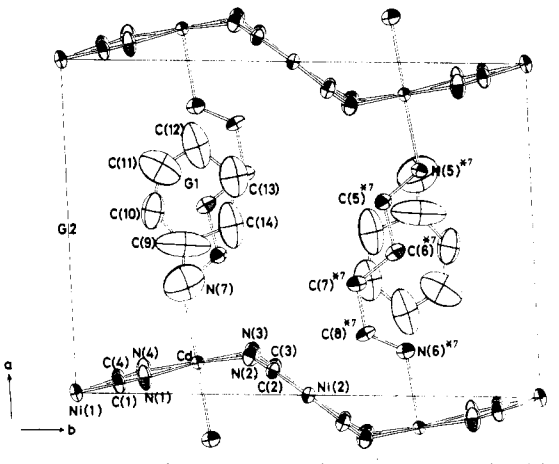

Figure 3. Projection of the structure of **2** along the c axis with the numbering scheme. See the key to symmetry operations in Table VI for the asterisked number. 30% thermal ellipsoids are shown; hydrogen atoms are omitted.

and the nitrogens of the cyano groups to give a folded structure of the sheet. The waved sheets are stacked along the a axis of the crystal with the supporting "columns" of dabn providing cavities for guest molecules.

This fundamental structure shows the variation of the geometry in detailed parts on changing the guest from one to another. We can assume a cavity unit of a parallelepiped capped with two meshes of the cyanometal complex sheets above and beneath as shown in Figure 7. The unit is not always occupied by guest

Table IV. Final Atomic Parameters for **3**

	G^a	x/a	y/b	z/c	$B_{eq}/Å^{2\,b,c}$
Cd	0.5	0.02612 (5)	0.25	0.00379 (7)	2.00 (1)
Ni	0.5	0.0	0.0	0.5	2.02 (2)
C(1)	1.0	−0.0168 (5)	0.0885 (3)	0.3164 (6)	2.5 (2)
C(2)	1.0	0.0479 (5)	0.0852 (3)	0.6964 (6)	2.5 (1)
C(3)	0.5	0.3881 (8)	0.25	0.134 (1)	4.7 (4)
C(4)	0.5	0.545 (1)	0.25	0.261 (2)	8.2 (7)
C(5)	0.5	0.589 (1)	0.25	0.462 (1)	5.1 (4)
C(6)	0.5	0.7478 (9)	0.25	0.586 (1)	5.2 (4)
C(7)	0.5	0.5	0.0	0.5	5.0
C(8)	0.5	0.354 (1)	0.0198 (9)	0.405 (2)	5.0
C(9)	1.0	0.2983 (7)	−0.0188 (4)	0.193 (1)	5.0
C(10)	0.5	0.390 (1)	−0.054 (1)	0.130 (2)	5.0
C(11)	1.0	0.5467 (7)	−0.0749 (5)	0.234 (1)	5.0
C(12)	0.5	0.609 (1)	−0.034 (1)	0.446 (2)	5.0
N(1)	1.0	−0.0243 (5)	0.1423 (3)	0.2070 (7)	3.7 (2)
N(2)	1.0	0.0730 (5)	0.1373 (3)	0.8132 (6)	3.4 (1)
N(3)	0.5	0.2674 (7)	0.25	0.204 (1)	4.9 (3)
N(4)	0.5	0.7826 (6)	0.25	0.7928 (9)	4.1 (3)
N(5)	0.5	0.562 (1)	0.0427 (8)	0.723 (2)	5.0
H(1)[d]	1.0	0.2839	0.1924	0.2944	5.0
H(2)	1.0	0.3730	0.1924	0.0439	5.0
H(3)	1.0	0.5880	0.1924	0.2033	5.0
H(4)	1.0	0.5347	0.1924	0.5099	5.0
H(5)	1.0	0.7914	0.1924	0.5433	5.0
H(6)	1.0	0.7296	0.1924	0.8254	5.0

[a] G: multiplicity. [b] $B_{eq} = 4(\sum_i\sum_j B_{ij}a_ia_j)/3$. [c] The isotropic thermal parameter B was fixed at 5.0 Å^2 for C(7)–C(12), N(5), and H(1)–H(6) in the refinement. [d] H(1) at N(3), H(2) at C(3), H(3) at C(4), H(4) at C(5), H(5) at C(6), and H(6) at N(4).

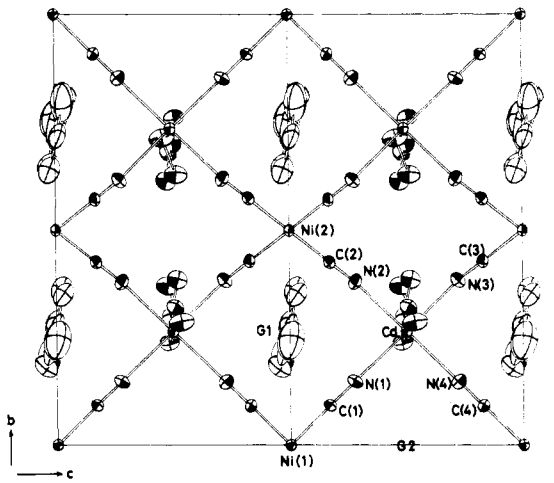

Figure 4. Projection of the structure of **2** along the a axis.

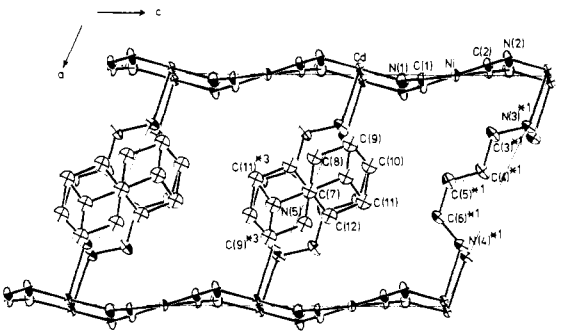

Figure 5. Projection of the structure of **3** along the b axis with the numbering scheme. See the key to symmetry operations in Table VII for the asterisked number. 30% thermal ellipsoids are shown for the host atoms and isotropic spheres of 5.0 Å^2 for the guest atoms; hydrogen atoms are omitted. One orientation of *N,N*-dimethylaniline molecule is given by C(8)–C(9)–C(10)–C(11)–C(12)–C(7)–N(5)–C(9)*3–C(11)*3 and another by C(12)*3–C(11)*3–C(10)*3–C(9)*3–C(8)*3–C(7)–N(5)*3–C(9)–C(11); the position of each atom with *3 is interrelated with that of the normal one by the inversion center where C(7) is located.

Table V. Selected Atomic Distances (Å) and Angles (deg) for **1**[a]

Cd–N(1)	2.323 (4)	Cd–N(2)	2.353 (5)
C(1)–N(2)	1.142 (5)	Ni–C(1)	1.848 (4)
N(2)–C(2)	1.472 (7)	C(2)–C(3)	1.522 (8)
C(3)–C(3)*[1]	1.522 (7)		
C(1)–Ni–C(1)*[2]	90.7 (2)	C(1)–Ni–C(1)*[3]	89.3 (2)
Ni–C(1)–N(1)	177.6 (3)	C(1)–N(1)–Cd	157.6 (3)
N(1)–Cd–N(2)	88.7 (1)	N(1)–Cd–N(1)*[4]	91.3 (1)
N(2)–Cd–N(1)*[4]	91.3 (1)	Cd–N(2)–C(2)	119.6 (4)
N(2)–C(2)–C(3)	115.3 (5)	C(2)–C(3)–C(4)*[1]	111.8 (5)

[a] Key to symmetry operations: normal, x, y, z; with *1, $1-x, -y, 1-z$; with *2, $x, 1-y, z$; with *3, $-x, y, 1-z$; with *4, $-x, y, -z$.

Table VI. Selected Atomic Distances (Å) and Angles (deg) and the Least-Squares Plane of the Aniline Molecule for **2**[a]

Cd–N(1)	2.387 (9)	Cd–N(2)	2.382 (9)
Cd–N(3)	2.382 (9)	Cd–N(4)	2.353 (9)
Cd–N(5)	2.271 (9)	Cd–N(6)*[1]	2.31 (1)
C(1)–N(1)	1.13 (1)	C(2)–N(2)	1.15 (1)
C(3)–N(3)	1.14 (1)	C(4)–N(4)	1.15 (1)
C(1)–Ni(1)	1.855 (9)	C(2)–Ni(2)	1.854 (9)
C(3)–Ni(2)*[2]	1.85 (1)	C(4)–Ni(1)*[2]	1.862 (9)
N(5)–C(5)	1.45 (1)	C(5)–C(6)	1.53 (2)
C(6)–C(7)	1.50 (2)	C(7)–C(8)	1.53 (2)
C(8)–N(6)	1.38 (2)	N(7)–C(9)	1.13 (4)
C(9)–C(10)	1.37 (5)	C(10)–C(11)	1.28 (4)
C(11)–C(12)	1.28 (5)	C(12)–C(13)	1.48 (4)
C(13)–C(14)	1.43 (5)	C(14)–C(9)	1.57 (5)
N(1)–Cd–N(2)	86.9 (3)	N(2)–Cd–N(3)	92.1 (3)
N(3)–Cd–N(4)	88.2 (3)	N(4)–Cd–N(1)	92.7 (3)
N(5)–Cd–N(1)	89.8 (3)	N(5)–Cd–N(2)	90.9 (3)
N(5)–Cd–N(3)	93.2 (3)	N(5)–Cd–N(4)	90.6 (3)
N(6)*[1]–Cd–N(1)	91.5 (3)	N(6)*[1]–Cd–N(2)	92.5 (3)
N(6)*[1]–Cd–N(3)	85.5 (3)	N(6)*[1]–Cd–N(4)	86.0 (3)
C(1)–Ni(1)–C(4)*[3]	90.5 (4)	C(1)–Ni(1)–C(4)*[4]	95.1 (4)
C(2)–Ni(1)–C(3)*[3]	90.9 (4)	C(2)–Ni(1)–C(3)*[5]	89.1 (4)
Ni(1)–C(1)–N(1)	179.1 (9)	C(1)–N(1)–Cd	178.3 (8)
Ni(2)–C(2)–N(2)	177.7 (9)	C(2)–N(2)–Cd	154.4 (8)
Ni(2)*[2]–C(3)–N(3)	178.0 (9)	C(3)–N(3)–Cd	147.5 (8)
Ni(1)*[2]–C(4)–N(4)	179.2 (9)	C(4)–N(4)–Cd	173.6 (8)
Cd–N(5)–C(5)	117.4 (7)	N(5)–C(5)–C(6)	115 (1)
C(5)–C(6)–C(7)	113 (1)	C(6)–C(7)–C(8)	115 (1)
C(7)–C(8)–N(6)	116 (1)	C(8)–N(6)–Cd*[6]	117.9 (8)
N(7)–C(9)–C(10)	139 (4)	N(7)–C(9)–C(14)	108 (4)
C(14)–C(9)–C(10)	113 (2)	C(9)–C(10)–C(11)	125 (3)
C(10)–C(11)–C(12)	131 (4)	C(11)–C(12)–C(13)	111 (3)
C(12)–C(13)–C(14)	126 (3)	C(13)–C(14)–C(9)	114 (3)

plane	N(7), C(9), C(10), C(11), C(12), C(13), C(14)
equation	$0.04359X - 0.22072Y + 0.97436Z + 0.63250 = 0$[b]
deviation/Å	N(7), 0.04696; C(9), −0.01537; C(10), −0.04134; C(11), 0.04427; C(12), 0.00152; C(13), −0.02636; C(14), −0.00001

[a] Key to symmetry operations: normal, x, y, z; with *1, $-1+x, y, z$; with *2, $x, y, 1+z$; with *3, $x, y, -1+z$; with *4, $-x, -y, 1-z$; with *5, $-x, 1-y, 1-z$; with *6, $1+x, y, z$; with *7, $1-x, 1-y, 1-z$. [b] The orthogonal coordinates are defined as

$$\begin{pmatrix} X \\ Y \\ Z \end{pmatrix} = \begin{pmatrix} a & b\cos\gamma & c\cos\beta \\ 0 & b\sin\gamma & -c\cos\alpha^* \sin\beta \\ 0 & 0 & 1/c^* \end{pmatrix} \begin{pmatrix} x \\ y \\ z \end{pmatrix}$$

molecule but in some cases by parts of the bridging ligands. Since two cavity units are formed for one formula unit of the host metal complex, the ratio of the cavity units occupied by guests to those by the bridging ligands rules the stoichiometric coefficient n in the compositional formula $Cd(dabn)Ni(CN)_4 \cdot nG$.

Pyrrole Compound (1). The skeletal chain of dabn ligand in a trans–trans conformation bridges adjacent cyanometal complex sheets across the *ac* plane of the unit cell cornered by Cd atoms. The distance between adjacent sheets, i.e. the basal spacing between the cyanometal complex sheets, becomes 7.840 Å, although the length of the dabn bridge is 10.54 Å. The sheets with a bending angle of 22.4° at Cd–N(1)–C(1), the value being the supplementary angle of the C(1)–N(1)–Cd angle in Table VI, are stacked along the *a* axis of the crystal to provide a cavity centered at $(1/2, 1/2, 0)$ with the guest pyrrole molecule. Another cavity unit centered at $(1/2, 0, 1/2)$ is occupied by the bridging dabn itself. Thus the stoichiometric coefficient $n = 1$ is given.

The cavity can be seen to have a tunnellike character extended along the *c* axis of the crystal centered at $y/b = 1/2$. The tunnel is walled by the dabn columns at $y/b = 0$ and 1, and each cavity is compartmentalized by electron clouds of the cyanide groups at the top and the bottom. In this cavity the guest pyrrole molecule shows an apparent shape of a couple of pentagons sharing one edge and may have freedom of motion to a considerable extent.

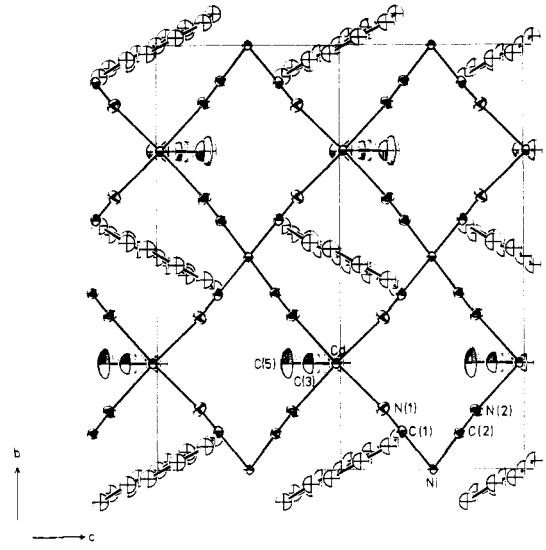

Figure 6. Projection of the structure of **3** along the *a* axis.

Table VII. Selected Atomic Distances (Å) and Angles (deg) and the Least-Squares Plane of the *N,N*-Dimethylaniline Molecule for **3**[a]

Ni–C(1)	1.871 (5)	Ni–C(2)	1.873 (5)
C(1)–N(1)	1.132 (7)	C(2)–N(2)	1.131 (7)
Cd–N(1)	2.374 (5)	Cd*[1]–N(2)	2.353 (4)
Cd–N(3)	2.315 (7)	Cd*[2]–N(4)	2.273 (7)
N(3)–C(3)	1.43 (1)	C(3)–C(4)	1.48 (1)
C(4)–C(5)	1.38 (2)	C(5)–C(6)	1.47 (1)
C(6)–N(4)	1.417 (9)	C(7)–C(8)	1.37 (1)
C(8)–C(9)	1.58 (2)	C(9)–C(10)	1.25 (1)
C(10)–C(11)	1.46 (1)	C(11)–C(12)	1.59 (1)
C(12)–C(7)	1.35 (1)	C(7)–N(5)	1.66 (1)
N(5)–C(9)*[3]	1.32 (1)	N(5)–C(11)*[3]	1.29 (1)
C(1)–Ni–C(2)	89.2 (5)	C(1)–Ni–C(2)*[4]	90.8 (2)
Ni–C(1)–N(1)	178.7 (5)	C(1)–N(1)–Cd	165.5 (4)
Ni–C(2)–N(2)	178.2 (5)	C(2)–N(2)–Cd*[1]	158.0 (4)
N(1)–Cd–N(1)*[5]	87.6 (2)	N(1)–Cd–N(2)*[6]	89.2 (1)
N(2)*[6]–Cd–N(2)*[7]	94.0 (1)	N(3)–Cd–N(1)	92.3 (2)
N(3)–Cd–N(2)*[6]	87.8 (2)	N(4)*[8]–Cd–N(1)	88.9 (2)
N(4)*[8]–Cd–N(2)*[6]	91.1 (2)	Cd–N(3)–C(3)	121.1 (5)
N(3)–C(3)–C(4)	117.5 (7)	C(3)–C(4)–C(5)	121.6 (9)
C(4)–C(5)–C(6)	123.0 (9)	C(5)–C(6)–N(4)	123.9 (9)
C(6)–N(4)–Cd*[2]	123.2 (6)	C(7)–C(8)–C(9)	110.6 (9)
C(8)–C(9)–C(10)	119 (1)	C(9)–C(10)–C(11)	130 (1)
C(10)–C(11)–C(12)	113.3 (9)	C(11)–C(12)–C(7)	111 (1)
C(12)–C(7)–C(8)	135.0 (8)	C(8)–C(7)–N(5)	111.3 (7)
C(12)–C(7)–N(5)	1127.7 (7)	C(7)–N(5)–C(9)*[3]	108.4 (8)
C(7)–N(5)–C(11)*[3]	110.3 (8)	C(9)*[3]–N(5)–C(11)*[3]	140 (1)

plane	N(5), C(7), C(8), C(9), C(10), C(11), C(12)
equation	$-0.03257X + 0.86937Y + 0.49308Z + 0.21462 = 0$
deviation/Å	N(5), −0.01906; C(7), 0.05405; C(8), 0.00644; C(9), 0.03079; C(10), −0.02466; C(11), 0.03012; C(12), −0.05697

[a] Key to symmetry operations: normal, x, y, z; with *1, $x, y, 1+z$; with *2, $1+x, y, z$; with *3, $1-x, -y, -z$; with *4, $-x, -y, 1-z$; with *5, $x, 1/2-y, z$; with *6, $x, y, -1+z$; with *7, $x, 1/2-y, -1+z$; with *8, $-1+x, y, z$; with *9, $1-x, -y, 1-z$.

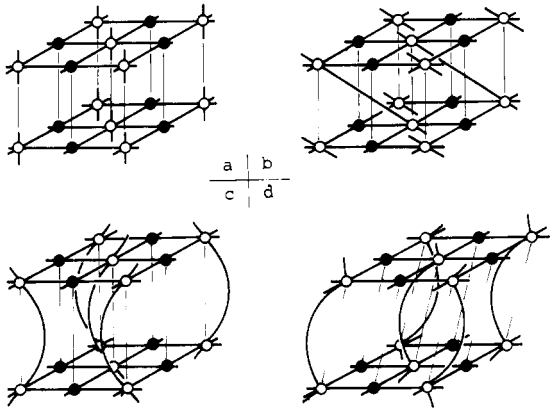

Figure 7. Models of cavity unit, four units shown for each model: (a) Hofmann-type and Hofmann-en-type, every cavity unit occupied by guest; (b) **1**, two cavity units occupied by dabn bridges and two by guests, respectively; (c) **2**, a cavity unit occupied by two dabn bridges and the remaining three by guests; (d) **3**, two cavity units occupied by dabn bridges and two by guests, respectively.

As the thermal parameters have been fixed at 5.0 Å^2 in the process of refinement, we cannot discuss the motion of the guest in detail on the basis of the present data. No anomalous bond lengths and angles have been observed for the host moieties except the bending angle in the cyanometal complex sheet; the angles are compared with each other for the four compounds later.

Aniline Compound (2). The dabn ligand bridging adjacent cyanometal complex sheets is in a cis–trans conformation similar to those observed for **3** and the Hofmann-dabn-type 2,5-xylidine compound $Cd[NH_2(CH_2)_4]Ni(CN)_4$·2,5-$(CH_3)_2C_6H_3NH_2$ (**4**) previously reported.[3] As shown in Figure 3, the cyanometal complex sheet bends unsymmetrically about the Cd atom; one side is almost linear with angles of 1.7 (Cd–N(1)–C(1)) and 6.4° (Cd–N(4)–C(4)), but another side is steeply bent with angles of 25.6 (Cd–N(2)–C(2)) and 32.5° (Cd–N(3)–C(3)). Thus the unit cell is doubled along the *b* axis of the crystal and affords four cavity units. As one of the four cavity units, centered at ($^1/_2$, $^1/_2$, $^1/_2$), is occupied by the dabn ligands, three are available for the guest molecules. The coefficient n = 1.5 in the compositional formula of **2** is consistent with this structure. Although the G1 aniline molecule in the cavity centered at ($^1/_2$, $^1/_4$, 0) (and the equivalent point ($^1/_2$, $^3/_4$, 0)) revealed its molecular structure in the refinement process, G2 in the cavity centered at ($^1/_2$, 0, $^1/_2$) did not. As shown in Figures 3 and 4, G1 is accommodated between the cyanometal complex sheets with its molecular axis almost parallel to the dabn bridge; the aromatic plane of G1, distributed within 0.05 Å from the least-squares plane, is slightly inclined to the *ab* plane of the crystal. The large thermal amplitude of each skeletal atom of G1 extending along its aromatic plane suggests the large extent of freedom of reorientational motion within the plane. The G2 aniline appears to take highly disordered orientations or vigorous motions: the refinement of the positional and thermal parameters was impossible even for the skeletal atoms.

The length of the dabn bridge in the cis–trans conformation is shortened to 9.774 Å by 0.77 Å from the 10.54-Å value for **1** in the trans–trans conformation, but the basal spacing, being approximated to 9.7 Å ($=a \sin \beta$), is expanded by 1.9 Å from the 7.840-Å value of **1**, owing to the accommodation of an aniline molecule larger than the pyrrole one. The 9.7-Å spacing in **2** is longer by ca. 1.1 Å than that observed for the Hofmann-type aniline clathrate $Cd(NH_3)_2Ni(CN)_4$·$2C_6H_5NH_2$.[2] The distance between the N(7) atom of G1 aniline and the amino nitrogen of dabn (N(5)), 3.72 (3) Å, appears too long for a hydrogen bond between the guest and the host; the shortest distance between the host and the guest is 3.54 (3) Å for N(7)–N(4), the N(4) being a cyano nitrogen in the cyanometal complex sheet.

***N,N*-Dimethylaniline Compound (3).** The structure of **3** is essentially similar to that of **4**. The dabn bridge takes a cis–trans conformation with a length of 9.860 Å, the value being slightly longer than that of 9.795 Å in **4** and giving the basal spacing of 9.01 Å. The bending angles in the cyanometal complex sheet are 14.5 at N(1) and 22.0° at N(2), respectively, and are considerably smaller than those observed in **2** and those (14.8 and 35.1°) in **4**. The cavity centered at ($^1/_2$, 0, 0) (and the equivalent position) is occupied by the guest molecule but that at ($^1/_2$, $^1/_4$, $^1/_2$) (and the equivalent position) is occupied by the dabn ligand, the 1:1 ratio leading to the stoichiometry of the compositional formula.

The dabn ligands arranged on the *ac* plane make up the wall of the tunnellike cavity extended along the *c* axis of the crystal, the cavity in which the guest molecule shows a large angle of inclination, 25.9°, between the aromatic plane and the *c* axis, the assumed molecular structure being considerably distorted along the aromatic plane. Although it should be unreasonable that the dimethylamino group was coplanar to the aromatic plane, a more reasonable model could not be derived from the present experimental data at room temperature. The shortest distance between the host and the guest is 3.56 (1) Å for C(9)–N(3), and that between the guests is 3.52 (2) Å for C(10)–C(1)*[9].

Discussion

Our first attempt to develop a three-dimensional host from the two-dimensional Hofmann-type was materialized in the crystal structure of the Hofmann-en-type clathrate $Cd(en)Ni(CN)_4$·2G[8,9] where en refers to ethylenediamine, or 1,2-diaminoethane, the shortest α,ω-diaminoalkane so far applied to the modification of a Hofmann-type host. In the Hofmann-en-type host, the size of the guest is limited to that not larger than benzene because of the ca. 8-Å span length of the en bridge between the cyanometal complex sheets. The shape of the cavity for the guest is similar to that in the Hofmann type. Since the host of the Hofmann-type clathrate $M(NH_3)_2M'(CN)_4$·2G (M = Mn, Fe, Co, Ni, Cu, Zn, or Cd; M′ = Ni, Pd, or Pt) has a layered structure stacked with a coplanar two-dimensional network of *catena*-[M(II)-metal tetrakis(μ-cyano)M′(II)-metalate], the basal spacing is only the dominant variable for accommodating various guests into the interlayer cavities. The value of basal spacing has range from the shortest, 7.98 Å for Ni–Ni–pyrrole (M = Ni, M′ = Ni, and G = pyrrole), to the longest, 12.65 Å for Ni–Ni–biphenyl.[2] Similarly, the flexibility of the Hofmann-en-type host has been observed only for the decrease of the basal spacing by change of the guest from benzene (8.06 Å) or thiophene (7.90 Å) to pyrrole (7.86 Å).[2] On the other hand, the Hofmann-dabn-type Cd(dabn)$Ni(CN)_4$ host is more flexible than the Hofmann-en-type for accommodating the guest molecules with various shapes and sizes. For the Hofmann-dabn-type we can define three variables that govern the crystal structure, i.e., the geometry of the cavity for the guest molecule to a first approximation: the conformation of dabn ligand, the basal spacing, and the bending angle in the cyanometal complex network.

Assuming that a three-dimensional framework is built of coplanar sheets of $CdNi(CN)_4$ in the same dimensions as those observed for the Hofmann-type Cd–Ni–benzene clathrate and of bridging dabn in a trans–trans conformation, we obtain a model structure as shown in Figure 8a. Although this model appears to be favorable to the coordination structure without any distortion in bonding angles and lengths, accommodation of a real guest molecule cannot be expected with an effective packing. For the accommodation of the pyrrole molecule, the basal spacing of 9.8 Å is too long. Moreover, a gap is left between the columns of dabn ligands: there are big holes in the walls enclosing the cavities. The void spaces are filled up by the shift and moving up of, e.g., the bottom cyanometal complex sheet to the right-hand side accompanied with a greater inclination of dabn columns, the inclination that gives rise to the close molecular (van der Waals) contact between the dabn columns and the bending of the cyanometal complex sheet as exemplified in the real structure of **1** shown in Figure 8b. The bending of the metal complex sheet causes the contraction of the Cd–Cd distance from 7.575 Å in the model to 7.060 Å (the *c* dimension of unit cell), the contraction

(8) Iwamoto, T. *Inorg. Chim. Acta* **1968**, *2*, 269.
(9) Miyoshi, T.; Iwamoto, T.; Sasaki, Y. *Inorg. Chim. Acta* **1972**, *6*, 59.

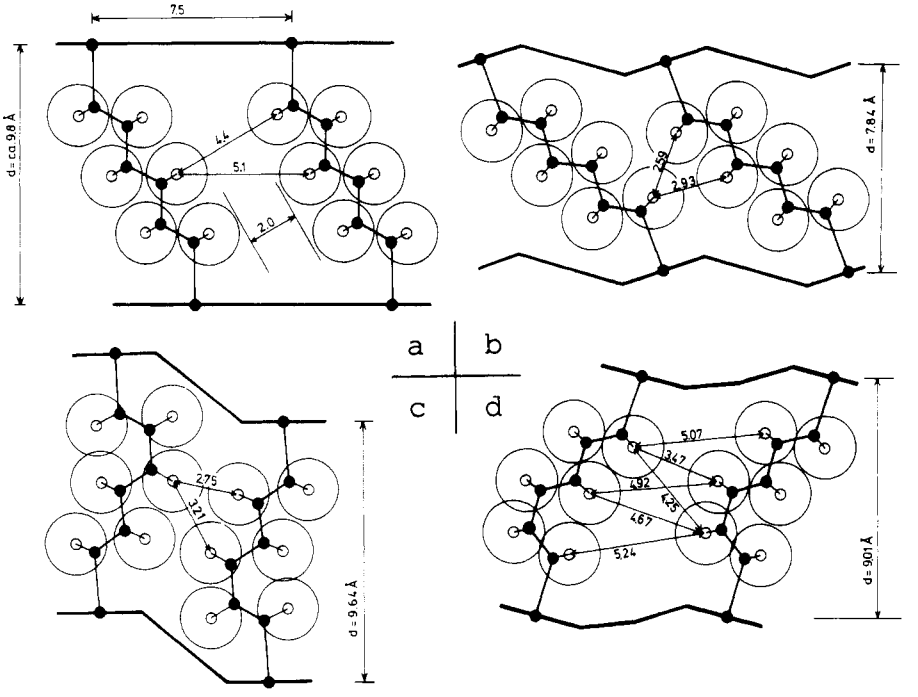

Figure 8. Flexibility of host structure: (a) hypothetical model with a trans–trans dabn bridge; (b) **1**; (c) **2**; (d) **3**.

being also favorable for accommodating the pyrrole molecule smaller than benzene.

The 9.8-Å spacing in the model structure seemed more than long enough to accommodate aniline molecule. However, the gap between the dabn columns, being unfavorable for the packing, should reappear if the inclination of the dabn column in the trans–trans conformation was recovered from **1**. As shown in Figure 8c, the structure of **2** with the dabn column of the cis–trans skeleton almost vertical to the metal complex sheet is favorable to the van der Waals contact between the dabn columns. The bending of the metal complex sheet, on the other hand, occurs to a great extent; the Cd–Cd distance decreases to 6.96 Å ($=b/2$). The contracted Cd–Cd distance and the basal spacing of 9.75 Å provide a slim cavity with the G1 aniline molecule. Although the spacing of 9.75 Å appears to be longer than the minimum essential length for the aniline molecule, 8.66 Å observed for the Hofmann-type Cd–Ni–aniline,[2] the steep bending of the metal complex sheet makes the effective volume of the cavity smaller. The cavity for the G2 aniline molecule has the effective volume larger than that for G1 because the electron clouds of dabn ligand invading into this cavity are only those of the amino groups and the C(6) methylene group (see Figures 3 and 4).

In spite of the fact that the *N,N*-dimethylaniline molecule, being bulkier than aniline, is accommodated in **3**, the dabn bridge in the cis–trans conformation gives the basal spacing 9.01 Å ($a \sin \beta$), shorter by 0.74 Å than that observed for **2**; the less steep bending of the metal complex sheet makes a gap between the dabn columns. However, these factors are rather favorable to the accommodation of the *N,N*-dimethylaniline molecule. Although the basal spacing decreases, the 9.860-Å dabn bridge is long enough to hold the *N,N*-dimethylaniline molecule obliquely along the bridge in the unit cell with the monoclinic distortion. The aromatic plane of the guest is also arranged obliquely to the *c* axis of crystal so that the gap between the dabn columns is filled up with the methyl group of the guest molecule.

In this respect the structure of **3** is comparable with that of **4**, in which the monoclinic angle 105.56° is smaller by 8.38° and the dabn bridge length is shorter by 0.065 Å than those in **3**. The molecular shape of 2,5-xylidine with two methyl and one amino substituent groups is more favorable to the accommodation in the interlayer cavity of a Hofmann-dabn-type host. The amino group is held between the amino groups of dabn ligands by at least a hydrogen bond with one of the dabn amino groups; the gap between the dabn columns is efficiently filled up with the two methyl groups, one from each of the neighboring guest molecules. In the case of **3**, the gap is filled up with an average of one methyl group, and another methyl group is located near the position between the dabn amino groups without any hydrogen bonds. The disorder observed for the *N,N*-dimethylaniline molecule is caused from the less effective packing in the cavity compared with that of the 2,5-xylidine guest in **4**.

Acknowledgment. This work was supported by a Grant-in-Aid for the Special Project Research on the Properties of Molecular Assemblies (No. 58118007) from the Ministry of Education, Science and Culture.

Registry No. **1**, 100112-39-8; **2**, 100112-40-1; **3**, 100112-41-2.

Supplementary Material Available: Tables of anisotropic thermal parameters and structure factors for $Cd[NH_2(CH_2)_4NH_2]Ni(CN)_4 \cdot C_4H_5N$, $Cd[NH_2(CH_2)_4NH_2]Ni(CN)_4 \cdot 1.5C_6H_5NH_2$, and $Cd[NH_2(CH_2)_4NH_2]Ni(CN)_4 \cdot C_6H_5N(CH_3)_2$ (77 pages). Ordering information is given on any current masthead page.